Spectral phase reconstruction of femtosecond laser pulse from interferometric autocorrelation and evolutionary algorithm

J. Moreau, F. Billard, P. Béjot, E. Hertz

Spectral phase reconstruction of femtosecond laser pulse from interferometric autocorrelation and evolutionary algorithm

J. Moreau, F. Billard, P. Béjot, E. Hertz*

Laboratoire Interdisciplinaire Carnot de Bourgogne

UMR CNRS 6303 - Université Bourgogne Franche-Comté, 21078 Dijon Cedex, France

Abstract

We report on the complete temporal characterization of femtosecond laser pulses from second-order interferometric autocorrelation and laser spectrum measurements. The method exploits a newly developed autocorrelator based on a two photon-absorption signal produced directly within a camera sensor so as to provide a single-shot interferometric autocorrelation of great reliability and robustness. Interferometric autocorrelation trace and laser spectrum are exploited for a spectral phase retrieval via an evolutionary algorithm. The quality of the reconstruction for highly modulated spectral phases imprinted by a pulse shaper confirms the reliability of the method. The autocorrelator is compact, robust and easy to use. Possible improvements are discussed.

Keywords: Ultrafast laser pulse characterization; Pulse shaping; Evolutionary algorithm

1. Introduction

The development of ultrashort lasers has opened up a vast field of unexplored applications from THz to XUV spectral region. Many of these applications relies on the production of non-linear effects for which the matter response is extremely sensitive to the properties of the laser pulse and in particular to its temporal structure. The need of reliable and versatile diagnostic tools has therefore become extremely important [1–3]. There exists many characterization techniques for ultrashort laser pulses with varying experimental complexity, accuracy and limitation. Among them, the two most widely used comprehensive characterization techniques are frequency-resolved optical gating [3, 4] (FROG) and spectral phase interferometry for direct electric field reconstruction [3, 5] (SPIDER). These two methods provide a complete knowledge of the ultrashort laser pulse by reconstructing both the spectral (or temporal) amplitude and phase of the electric field. Several FROG [3, 4, 6–8] or SPIDER [3, 5, 9–11] variants have been developed to extend the scope of measurements. From an experimental point of view, the most popular and simple family of characterization methods remains the second-order autocorrelation where one can distinguish the intensity autocorrelation from the interferometric autocorrelation (IAC). IAC is a fringes resolved autocorrelation which contains more information than intensity autocorrelation but which can be less convenient to produce and analyze. Autocorrelation methods are commonly used in worldwide laboratories for a daily checking of laser systems. In their standard approach, these methods do not provide a complete characterization of the pulse but rather a rough measurement of its duration provided that a particular temporal pulse shape is assumed. Despite this limitation, autocorrelation techniques feature great advantages such as a low cost, an easy implementation and compactness of the device, and a low energy requirement (much lower than FROG or SPIDER). IAC also offers a self-calibration from fringes or a checking of the alignment from the contrast ratio. Furthermore, it has been shown that a better knowledge or even a complete characterization of the pulse can also be obtained from autocorrelation measurement when combined with additional information [12], overcoming the primary limitation of optical autocorrelators. Diels et al [13] have for instance used an unbalanced correlation, namely a cross correlation between the original pulse and one of its replica having experienced a known transformation as for instance a calibrated chirp. This method provides, under certain conditions, a complete characterization of the pulse. Another general class of methods is the so-called phase and inten-

*Corresponding author. e-mail:edouard.hertz@u-bourgogne.fr

sity from correlation and spectrum only [14, 15] (PICASO). PICASO requires the measurement of the pulse spectrum together with one (or more) nonlinear correlation, as for instance unbalanced intensity autocorrelation or IAC. On can notice that Naganuma *et al* [16] had already demonstrated about one decade before the advent of PICASO that IAC and pulse spectrum enables to uniquely retrieve the pulse through an assumption-free pulse reconstruction. While the convergence in the case of arbitrarily complex phase modulations was questioned at this time, Naganuma and co-workers paved the way for different experimental demonstration and several groups have successfully reported pulse reconstruction from multishot IAC and pulse spectrum by using different types of algorithms [17–19]. This method has nevertheless been gradually disregarded, probably because of the difficulty in obtaining both reliable IAC and spectrum measurements at the same time. We revisit in this work the strategy of Naganuma *et al* with a recently developed autocorrelator [20] called biprism based optical autocorrelation with retrieval (BOAR). This last provides a *single-shot* IAC trace of great reliability and robustness well-suited for a complete reconstruction of ultrashort pulses. By combining BOAR IAC and spectrum measurements with an evolutionary algorithm, we demonstrate the reconstruction of complex pulse shapes with a very good accuracy. To this end, laser pulses (70 fs duration and central wavelength λ_0=1450 nm) are spectrally phase-shaped via a standard pulse shaper device based on a liquid crystal display. Various complex phase modulations have been applied and retrieved with a great fidelity by means of this very compact and easy use device. Possible improvements of the method are discussed.

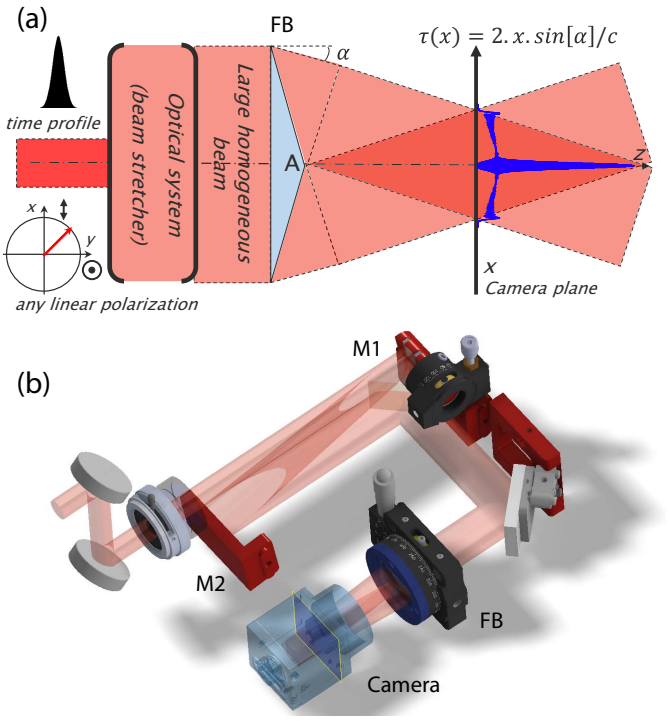

Figure 1. (a) Schematic description of the autocorrelator with FB the Fresnel biprism. The blue line in the plane of the camera corresponds to a typical two-photon absorption signal recorded by the camera. (b) BOAR set-up. M_1 et M_2: cylindrical mirror of -25 mm and +125 mm focal length respectively, FB: Fresnel biprism.

2. Description of the autocorrelator

As with any autocorrelator, the BOAR device relies on the production of two time-delayed replica of the pulse to be measured combined with a nonlinear optical effect. The heart of the device is composed of only two optical elements: a Fresnel biprism (FB) and a camera. The FB encodes the time delay into the transverse spatial dimension of the two crossing sub-beams recorded by the camera sensor for a single-shot operation. The camera is used as detector and nonlinear medium at the same time through the production of a two-photon absorption photocurrent.

The scheme of the device is depicted in Fig. 1. A cylindrical reflective telescope first increases the beam size by a factor of 5 in the horizontal direction on which the IAC measurement is encoded so as to ensure that the beam size will not limit the time window. After the telescope, the beam propagates through a 1.7 mm thick fused silica FB producing two identical beams crossing with an angle 2α:

$$\alpha = \text{asin}\left[n \times \sin(\frac{\pi - A}{2})\right], \quad (1)$$

where $A = 160.22°$ is the apex angle [20] and n the refractive index. In our case, $\alpha = 14.37°$. With such a beam geometry, the time delay is encoded into the spatial profile of the beam with a space-time conversion factor $\tau = \frac{2x \sin\alpha}{c}$ with x the distance with respect to the propagation axis z and c the celerity. The second-order autocorrelation is realized via a two photon-absorption signal produced directly within the CMOS sensor. If the bandgap of the sensor based semiconductor material is U_g, the signal recorded by the camera will rely on a two-photon absorption process for laser wavelength λ verifying $\frac{hc}{U_g} < \lambda < 2\frac{hc}{U_g}$. In the present case, the semiconductor material is Silicon with $U_g \approx 1.11$ eV so that the wavelength range of operation lies between 1200-2400 nm. This range is of particular interest for applications spanning from strong-field physics to optical telecommunications. The camera is located in the overlapping region of the two crossing beams. The 1.67 μm pixel size of the sensor allows to resolve the optical fringes in the whole spectral range while the 6.4 mm sensor size of the camera provides a temporal window of 3.5 ps. As explained in [20], special care has been taken to insure that the size of the biprism or the beam extension does not limit the latter in order to benefit from the full temporal window allowed by sensor size. The use of only two elements for this autocorrelator makes the BOAR extremely compact, calibration-free, robust in alignment and almost insensitive to the input polarization [20] since the nonlinear process is not limited by any phase matching consideration. The set-up is also very sensitive, typical input energy for a single-shot operation is 100 nJ.

3. Method

The spectral phase reconstruction of femtosecond laser pulse make use of two quantities: an IAC trace from the BOAR device and the pulse spectrum measured with an additional spectrometer. Suppose the electric field is written as $E(t) = A(t)e^{i\omega_0 t}$ with $\omega_0 = 2\pi c/\lambda_0$ the angular frequency and $A(t)$ the complex field envelope, the total complex electric field hitting a pixel of the camera is $E(t,\tau) = E_1(t) + E_2(t-\tau)$ with $E_1(t)$ (resp. $E_2(t)$) the field coming from the two faces of the biprism. The photocurrent I_{phot} induced by two-photon absorption on one pixel is therefore given by:

$$I_{\text{phot}}(\tau) \propto \int |E^2(t,\tau)|^2 dt. \quad (2)$$

The IAC signal is known to contain oscillating terms at $\omega \approx 0, \omega_0$ and $2\omega_0$ [16, 20] which (assuming a perfect balance between the two replicas amplitudes $A_1 = A_2 = A$) can write as:

$$I_{\text{phot}}(\tau) \propto 1 + 2G_2(\tau) + 2\mathcal{R}e\left[F_1(\tau)e^{-i\omega_0 t}\right] + \mathcal{R}e\left[F_2(\tau)e^{-2i\omega_0 t}\right] \quad (3)$$

with

$$G_2(\tau) = \int I(t)I(t-\tau)dt, \quad (4)$$

$$F_1(\tau) = \int [I(t) + I(t-\tau)]\, A(t)A^*(t-\tau)dt, \quad (5)$$

$$F_2(\tau) = \int A^2(t)A^{*2}(t-\tau)dt, \quad (6)$$

where the normalization $\int I^2(t)dt = 1$ has been used in the previous equations and where $I(t) = |A(t)|^2$ is the field intensity. The three oscillating contributions to the two-photon signal I_{phot} can be easily isolated by an appropriate spectral filtering. In the frequency domain, G_2, F_1 and F_2 are given by:

$$G_2(\omega) = |u(\omega)|^2, \quad (7)$$

$$F_1(\omega) = 2\mathcal{R}e\left[u(\omega) \otimes A(\omega)\right] A^*(\omega), \quad (8)$$

$$F_2(\omega) = |A_2(\omega)|^2. \quad (9)$$

where $u(\omega) = \mathcal{F}[I(t)]$, $A(\omega) = \mathcal{F}[A(t)]$ and $A_2(\omega) = \mathcal{F}\left[A^2(t)\right]$ with $\mathcal{F}$ the Fourier transform.

We call $\varphi(\omega)$ the spectral phase of the pulse to be characterized so that $A(\omega) = |A(\omega)|e^{i\varphi(\omega)}$. The spectral amplitude $|A(\omega)|$ is obtained from the measurement of the pulse spectrum $I(\omega) = |A(\omega)|^2$. From the knowledge of $|A(\omega)|$, an evolutionary algorithm is used to retrieve the spectral phase $\varphi(\omega)$ which best fits the experimental contributions $G_2(\omega)$, $F_1(\omega)$ and $F_2(\omega)$. The key ingredients of our algorithm have been already detailed elsewhere [21, 22]. Briefly, the spectrum and the spectral phase are sampled on a grid of 128 points. A spectral phase $\varphi(\omega)$ corresponds to one individual for the algorithm while the phase at a given frequency corresponds to the gene of the individual. The algorithm starts with a population of 900 individuals randomly selected to explore the whole search space but the population is reduced to 60 individuals from the second generation. Starting with the initial population, we calculate for each individual the differences:

$$\Delta G_2(\omega) = |G_2(\omega)| - \left|G_2^{exp}(\omega)\right|, \quad (10)$$

$$\Delta F_1(\omega) = |F_1(\omega)| - \left|F_1^{exp}(\omega)\right|, \quad (11)$$

$$\Delta F_2(\omega) = |F_2(\omega)| - \left|F_2^{exp}(\omega)\right|, \quad (12)$$

where $X_i(\omega)$ and $X_i^{exp}(\omega)$ are the optimized and the experimental contributions respectively. The fitness of each individual is then assessed by

$$S = -\int |\Delta G_2(\omega)| + R_1 |\Delta F_1(\omega)| + R_2 |\Delta F_2(\omega)|\ d\omega \quad (13)$$

where R_1 and R_2 are factors to confer the same weight to the three contributions in the fitness function. They are defined as:

$$R_1 = \frac{\int \left|G_2^{exp}(\omega)\right|\ d\omega}{\int \left|F_1^{exp}(\omega)\right|\ d\omega}, \quad (14)$$

$$R_2 = \frac{\int \left|G_2^{exp}(\omega)\right|\ d\omega}{\int \left|F_2^{exp}(\omega)\right|\ d\omega}. \quad (15)$$

$$(16)$$

For each new generation, the 10 best individuals (i.e. those maximizing S in Eq. 13) are cloned and the algorithm generates from these "parents" 50 new individuals or "children" with crossover and mutation. The mutation procedure is twofold. For a part of the children, the phase of very few genes (between 2 and 4%) is changed totally randomly while for the others, the phase of about 10% of the genes is muted by adding a random value within a range that is reduced along the optimization procedure. The algorithm thus produces a new population based on the success of the previous one and iteratively adjust the spectral phase to fit with the experimental measurements. Typical convergence is obtained within 200 generations taking less than 10 s on a standard laptop.

4. Results

Experiments are carried out with an optical laser source based on a Ti:sapphire chirped pulse amplifier delivering pulses of 100 fs duration, centered around 796 nm, at 1 kHz repetition rate. A NOPA (noncollinear optical parametric amplifier) generates the pulse of wavelength λ_0=1450 nm and duration 70 fs. The beam then pass through a standard pulse shaper device based on a programmable 1D dual mask LC-SLM array (SLM-320d from Jenoptik) within a $4f$ zero-dispersion line [23, 24] composed of a pair of diffraction gratings (600 grooves/mm) and a pair of cylindrical mirrors (400 mm focal length). The spectral sampling of the shaper has been measured to 55.9 GHz/pix leading to a temporal window [24] for the shaping $\Delta\tau = \pm 17.8$ ps. The device provides a full control over the spectral phase and amplitude of the field but phase shaping only was applied in this work. Various phase modulations have been applied with the pulse shaper and measured by the BOAR autocorrelator. IAC traces and measurement of the

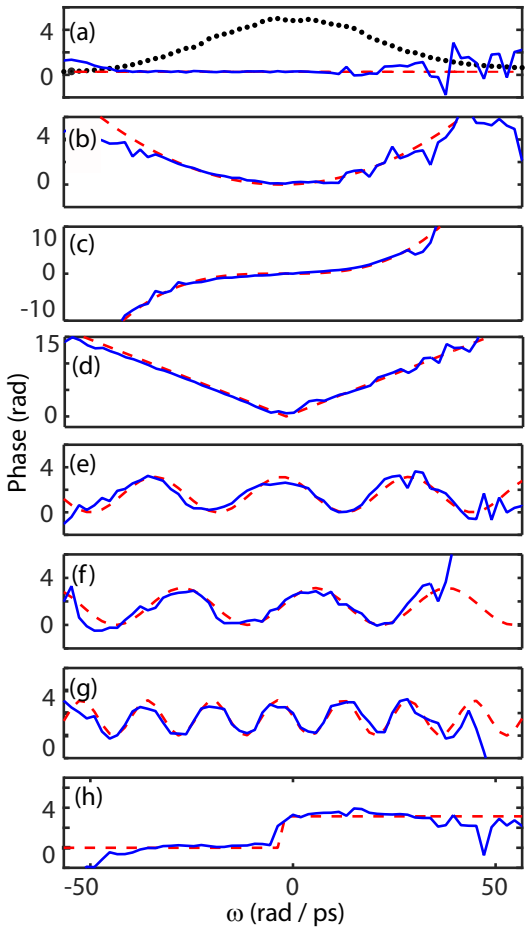

Figure 2. Characterization of spectral phases $\varphi(\omega)$ applied with the pulse shaper: (a) unshaped, (b) $\varphi(\omega) = \pm\phi^{(2)}/2(\omega-\omega_0)^2$ with $\phi^{(2)} = 6000$ fs^2, (c) $\varphi(\omega) = \pm\phi^{(3)}/6(\omega-\omega_0)^3$ with $\phi^{(3)} = 1\ 10^6$ fs^3, (d) triangular phase function of ±300 fs slope, (e) $\varphi(\omega) = \pi/2$ ([1+cos($\omega\tau$)] with $\tau = 200$ fs, (f) same as (e) but with sinus function, (g) same as (e) but with $\tau = 400$ fs, (h) π-phase jump. The red dashed lines depicts the phase encoded with the pulse shaper and the blue straight lines the phase retrieved by our device. The dotted black in (a) corresponds to the spectral amplitude.

pulse spectrum (with a resolution 1.2 THz) are used as input for the evolutionary algorithm to characterize the laser pulse as explained in the previous section. Main results, depicted in Fig. 2, demonstrate the relevance of our device to reconstruct very different spectral phases with a great fidelity. As shown, standard quadratic or cubic spectral phases have been characterized as well as with more exotic modulations such as sinusoidal or triangular phase functions. Even a phase step (Fig. 2(h)), which is notoriously difficult to characterize, has been relatively well reconstructed. It should be mentioned that the method features the same ambiguities as those of SHG FROG [4] and particularly the ambiguity of the direction of time (i.e. an ambiguity between $A(\omega)$ and $A(-\omega)$ in the frequency domain).

Fig. 3 shows the $|F_1|$, $|F_2|$ and $|G_2|$ contributions measured and optimized by the algorithm for some of the spectral phases presented in Fig. 2. As shown in Fig.3, these contributions present a very specific signature with the spectral phase enabling a good reconstruction of the latter. In addition to the shape, the relative amplitude is also an important parameter. Since the theoretical and experimental curves does not have necessarily the same amplitude, all the theoretical (resp. experimental) curves have been divided by max[$|G_2(\omega)|$] (resp. max$\left[\left|G_2^{exp}(\omega)\right|\right]$) for evaluating the difference used in the fitness function in Eq. 13. This global normalization factor (instead of an independent normalization of all the contributions) preserves the relative amplitude between G_2, F_1 and F_2 as depicted in Fig. 3. It turns out to be an additional useful criterion for the reconstruction of the spectral phase by the algorithm.

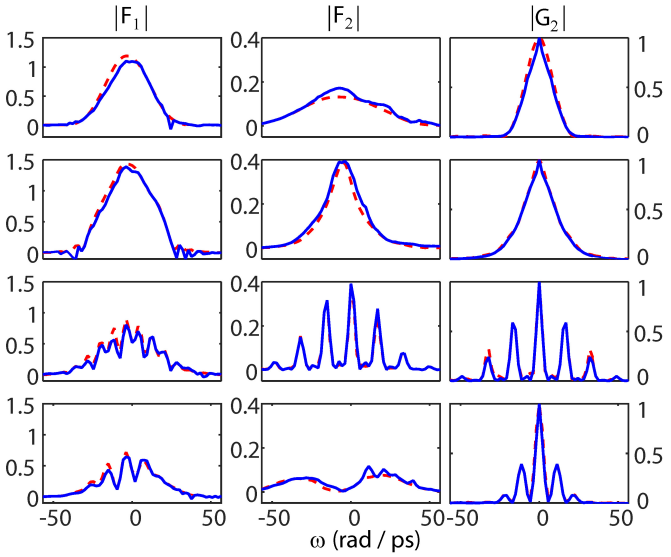

Figure 3. Left, middle and right columns: $|F_1|$, $|F_2|$ and $|G_2|$ contributions obtained from the measurements (red dashed line) and from the optimization by the algorithm (blue straight line) with different spectral phases. Upper line: quadratic spectral phase of Fig. 2(b), second line: cubic spectral phase of Fig. 2(c), third line: cosinus spectral phase of Fig. 2(g) and lower line: triangular phase of Fig. 2(d).

5. Conclusion

We have reported the complete characterization of femtosecond laser pulse from the combined measurement of single shot interferometric autocorrelation and laser spectrum. The autocorrelator is extremely compact, robust in alignment and the performance of the overall set-up for the spectral phase reconstruction is of high quality. The technique could be further improved in several ways. First of all, the wavelength range of operation between 1200-2400 nm with a Silicon camera could be extended in the SWIR region with an InGaAs camera (from 1800 to 3400 nm). The use of three-photon instead of two photon-absorption signal can also be envisioned for a low cost applicability in the deep-infrared. The present device is already extremely sensitive but it could be even improved by focusing the beam in the axis perpendicular to the direction on which the IAC measurement is encoded. This

could allow the measurement of pulses from fiber lasers. The present "unfocused" arrangement also offer the possibility of measuring the radial group delay dispersion, a spatio-temporal coupling occurring from a misalignment of grating compressor or affecting a laser beam propagating through prisms or lenses. Finally, the measurement of the pulse spectrum is performed in the present work via an additional spectrometer but this measurement could be integrated to the device. For instance, a dual one and two-photon detection could be used since a linear interferometric autocorrelation give access to the spectrum. Another possibility could be to spread spatially the different frequencies (via a grating for instance) and to measure it directly with the two-photon absorption mechanism in the camera so as to provide the squared spectral intensity.

Acknowledgement

This work has benefited from the facilities of the SMART-LIGHT platform in Bourgogne Franche-Comté (EQUIPEX+ contract "ANR-21-ESRE-0040"). This work has been supported by the EIPHI Graduate School (contract ANR-17-EURE-0002), Bourgogne-Franche-Comté Region, the CNRS, and the SATT Grand-Est.

References

[1] C. Rullière (Ed.), Femtosecond Laser Pulses, Springer-Verlag Berlin Heidelberg, 1998.

[2] A. Monmayrant, S. Weber, B. Chatel, A newcomer's guide to ultrashort pulse shaping and characterization, Journal of Physics B: Atomic, Molecular and Optical Physics 43 (10) (2010) 103001–.

[3] I. A. Walmsley, C. Dorrer, Characterization of ultrashort electromagnetic pulses, Adv. Opt. Photon. 1 (2) (2009) 308–437.

[4] R. Trebino, K. W. DeLong, D. Fittinghoff, J. Sweetser, M. A. Krumbügel, B. Richman, D. Kane, Measuring ultrashort laser pulses in the time-frequency domain using frequency-resolved optical gating, Review of Scientific Instruments 68 (1997) 3277–3295.

[5] C. Iaconis, I. A. Walmsley, Spectral phase interferometry for direct electric-field reconstruction of ultrashort optical pulses, Opt. Lett. 23 (10) (1998) 792–794.

[6] T. Nagy, P. Simon, Single-shot tg frog for the characterization of ultrashort duv pulses, Opt. Express 17 (10) (2009) 8144–8151.

[7] S. Linden, J. Kuhl, H. Giessen, Amplitude and phase characterization of weak blue ultrashort pulses by downconversion, Opt. Lett. 24 (8) (1999) 569–571.

[8] D. J. Kane, A. J. Taylor, R. Trebino, K. W. DeLong, Single-shot measurement of the intensity and phase of a femtosecond uv laser pulse with frequency-resolved optical gating, Opt. Lett. 19 (14) (1994) 1061–1063.

[9] P. Londero, M. E. Anderson, C. Radzewicz, C. Iaconis, I. A. Walmsley, Measuring ultrafast pulses in the near-ultraviolet using spectral phase interferometry for direct electric field reconstruction, Journal of Modern Optics 50 (2) (2003) 179–184.

[10] S. Birkholz, G. Steinmeyer, S. Koke, D. Gerth, S. Bürger, B. Hofmann, Phase retrieval via regularization in self-diffraction-based spectral interferometry, J. Opt. Soc. Am. B 32 (5) (2015) 983–992.

[11] P. Béjot, E. Szmygel, A. Dubrouil, F. Billard, B. Lavorel, Faucher, E. Hertz, Doppler effect as a tool for ultrashort electric field reconstruction, Opt. Lett. 45 (24) (2020) 6795–6798.

[12] J.-C. M. Diels, J. J. Fontaine, I. C. McMichael, F. Simoni, Control and measurement of ultrashort pulse shapes (in amplitude and phase) with femtosecond accuracy, Appl. Opt. 24 (9) (1985) 1270–1282.

[13] C. Yan, J.-C. Diels, Amplitude and phase recording of ultrashort pulses, J. Opt. Soc. Am. B 8 (6) (1991) 1259–1263.

[14] J. W. Nicholson, J. Jasapara, W. Rudolph, F. G. Omenetto, A. J. Taylor, Full-field characterization of femtosecond pulses by spectrum and cross-correlation measurements, Opt. Lett. 24 (23) (1999) 1774–1776.

[15] J. W. Nicholson, W. Rudolph, Noise sensitivity and accuracy of femtosecond pulse retrieval by phase and intensity from correlation and spectrum only (picaso), J. Opt. Soc. Am. B 19 (2) (2002) 330–339.

[16] K. Naganuma, K. Mogi, H. Yamada, General method for ultrashort light pulse chirp measurement, IEEE Journal of Quantum Electronics 25 (6) (June 1989) 1225–1233.

[17] K.-H. Hong, Y. S. Lee, C. H. Nam, Electric-field reconstruction of femtosecond laser pulses from interferometric autocorrelation using an evolutionary algorithm, Optics Communications 271 (1) (2007) 169–177.

[18] W. Yang, M. Springer, J. Strohaber, A. Kolomenski, H. Schuessler, G. Kattawar, A. Sokolov, Spectral phase retrieval from interferometric autocorrelation by a combination of graduated optimization and genetic algorithms, Opt. Express 18 (14) (2010) 15028–15038.

[19] N. F. Kleimeier, T. Haarlammert, H. Witte, U. Schühle, J.-F. Hochedez, A. BenMoussa, H. Zacharias, Autocorrelation and phase retrieval in the uv using two-photon absorption in diamond pin photodiodes, Opt. Express 18 (7) (2010) 6945–6956.

[20] F. Billard, A. Dubrouil, E. Hertz, S. Lecorné, E. Szmygel, O. Faucher, P. Béjot, Boar: Biprism based optical autocorrelation with retrieval, Review of Scientific Instruments 90 (6) (2019) 063110–.

[21] E. Hertz, A. Rouzée, S. Guérin, B. Lavorel, O. Faucher, Optimization of field-free molecular alignment by phase-shaped laser pulses, Phys. Rev. A 75 (3) (2007) 031403.

[22] A. Rouzée, E. Hertz, B. Lavorel, O. Faucher, Towards the adaptive optimization of field-free molecular alignment, Journal of Physics B-atomic Molecular and Optical Physics 41 (7) (2008) 074002.

[23] A. M. Weiner, Femtosecond pulse shaping using spatial light modulators, Review of Scientific Instruments 71 (5) (2000) 1929–1960.

[24] E. Hertz, F. Billard, G. Karras, P. Béjot, B. Lavorel, O. Faucher, Shaping of ultraviolet femtosecond laser pulses by fourier domain harmonic generation, Opt. Express 24 (24) (2016) 27702–27714.